Supporting Information

Multi-olefin containing polyethers and triazolinediones: a powerful alliance

Tobias Johann,[a] Hannes A. Houck,[b] Thi Dinh,[a] Ulrike Kemmer-Jonas,[a] Filip E. Du Prez[b] and Holger Frey[a,*]

*[a] Institute of Organic Chemistry, Johannes Gutenberg University, Duesbergweg 10-14, 55124 Mainz, Germany. *hfrey@uni-mainz.de*
[b] Department of Organic and Macromolecular Chemistry, Polymer Chemistry Research Group, Ghent University, Krijgslaan 281 S4bis, B-9000 Ghent, Belgium

Table of contents

1. Studies on the reaction of furfuryl-containing polyethers with Phenyl-TAD

During preliminary studies on suitable polyether substrates for triazolinedione (TAD) modification, we investigated furan-based moieties that are amenable for Diels-Alder (DA) reaction with maleimides. In particular, furfuryl-based polyethers represent a well-known platform for DA-click with dienophiles.[1] TAD and maleimide possess a similar molecular structure. The main difference is the presence of an N=N double bond compared to the ene bond in maleimide, which greatly enhances the reactivity of TADs in terms of DA and Alder-Ene (AE) reaction. Hence, according to the procedure described for functionalization of furfuryl containing peptides with TADs[2] we performed the reaction of furfuryl alcohol initiated PEG (F-PEG, **Scheme S1I**) and furfuryl glycidyl ether (FGE)-PEG copolymers (P(FGE-*co*-EG)(**Scheme S1II**) with phenyl-TAD.

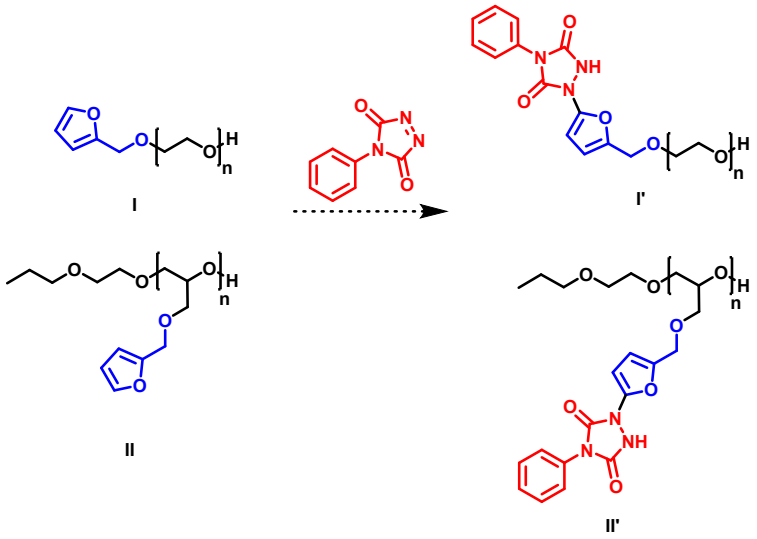

Scheme S1. Reaction of furfuryl alcohol initiated PEG (F-PEG, I) and furfuryl glycidyl ether (FGE) copolymers (P(FGE-co-EG)) with phenyl TAD. The furfuryl moieties (blue) were expected to undergo an AE reaction with phenyl-TAD (red) to yield the adducts shown (**I' and II'**)

However, unexpectedly copolymers containing multiple FGE units resulted in an ill-defined, insoluble material. In the case of F-PEG no protons of the furfuryl moiety can be detected via ^{1}H NMR characterization after reaction with an excess of phenyl-TAD ($\int d = 1 \rightarrow \int backbone = 600$). Additionally, comparing the integrals of the furfuryl moiety to the polyether backbone before ($\int aromatic H = 5 \rightarrow \int backbone = 65$) and after functionalization ( ) leads to the assumption that all protons (**Figure S1 a,b,c**) were substituted by phenyl TAD and a polymeric material is obtained. In the case of multiple furfuryl units per polymer chain (e.g. P(FGE-*co*-EG) copolymers) only a crosslinked, insoluble material is obtained. However, the exact mechanism of this reaction remains unknown from these preliminary studies.

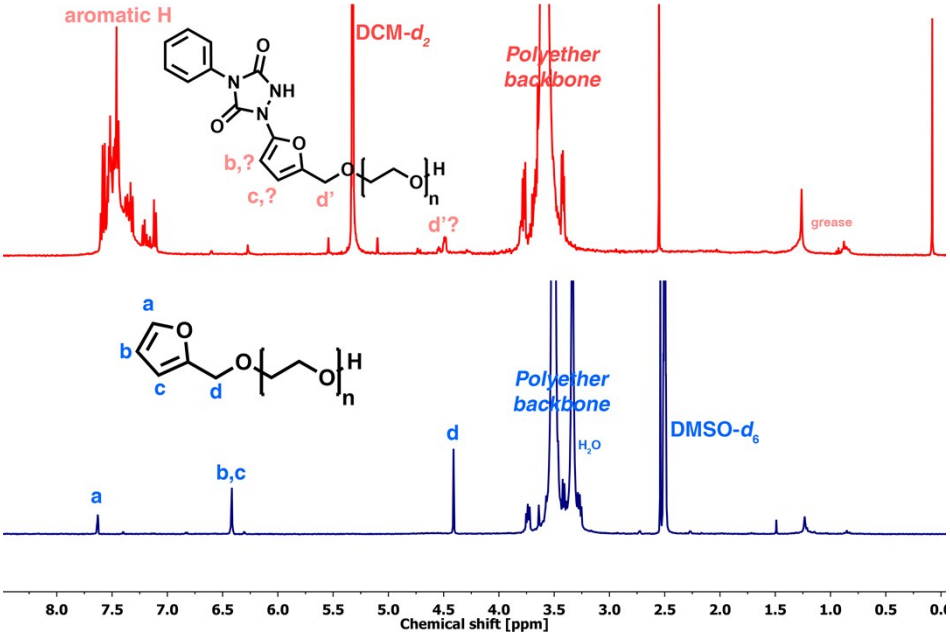

Figure S1. Stacked ^{1}H NMR spectra (300 MHz, DMSO-d_6, DCM-d_2) of F-PEG (bottom) and after reaction with phenyl-TAD (top). The characteristic signals of the furfuryl moiety cannot be detected anymore.

As an additionally model experiment 2-(methoxymethyl)furan was reacted with phenyl-TAD (**Scheme S2**). This model reaction was chosen, since it resembles only the furan moiety without any polymer repeating units.

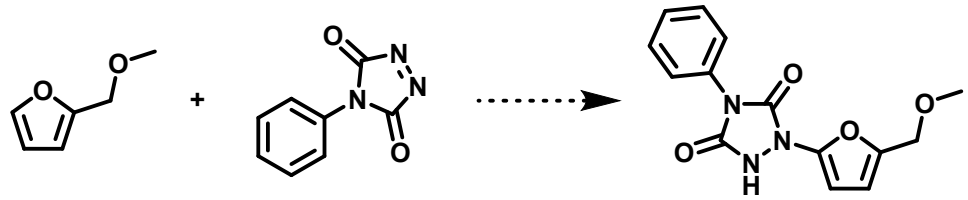

Scheme S2. Model reaction to analyse the reaction behaviour of furfuryl groups with phenyl TAD.

Analogous to the results obtained from the polymer samples, only an ill-defined sample was obtained. No signals of the furan moiety were assignable in ^{1}H NMR spectra (**Figure S2**). From these results it can be concluded that furfuryl ether based groups do not undergo selective reaction with phenyl-TAD. Multiple addition of TAD and even polymerization products are likely. Therefore, furfuryl-based polyethers are not suitable as a platform for TAD functionalization.

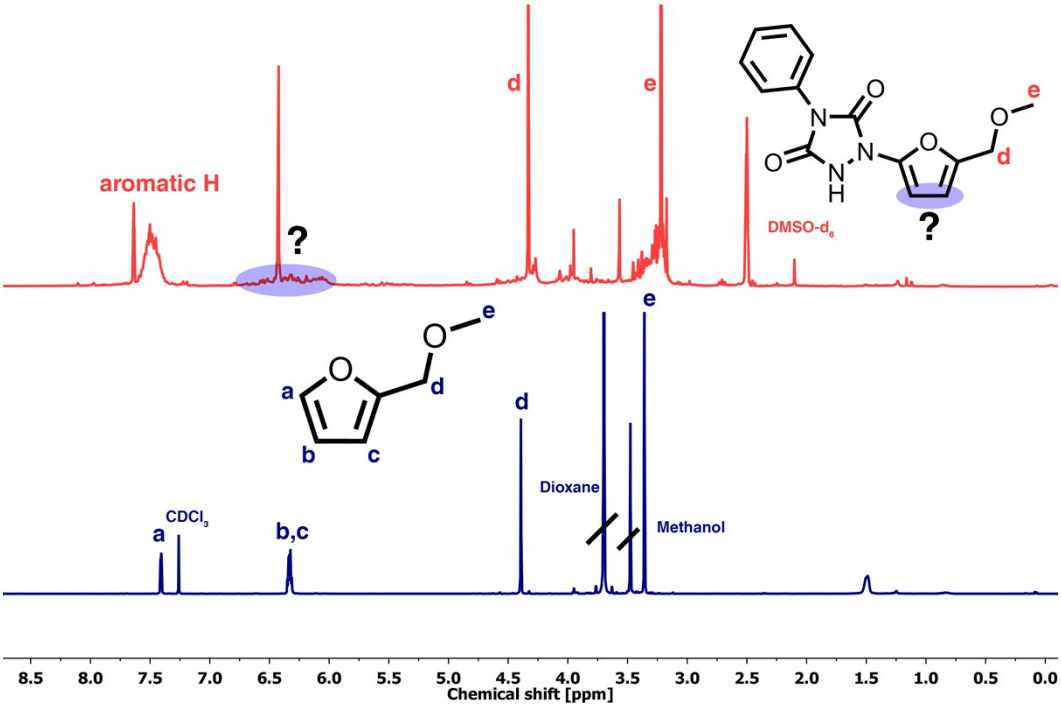

Figure S2. Stacked ^{1}H NMR spectra (300 MHz, $CDCl_3$, DMSO-d_6) of 2-(methoxymethyl)furan (bottom) and after reaction with phenyl-TAD (top). All signals (integrals, chemical shift) of 2-(methoxymethyl)furan are as expected. Note that extensive 2D NMR studies were performed to verify these results. However due to a lack of additional information these are not shown here.

2. Characterization data of HDEGE and CitroGE

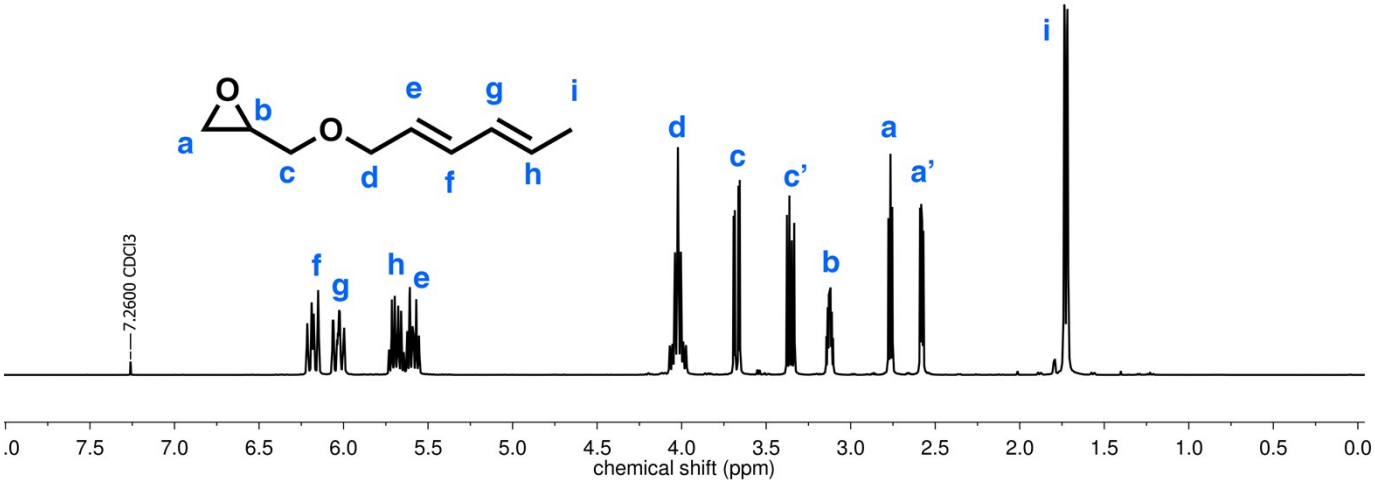

Figure S3a. ^{1}H NMR (400 MHz, $CDCl_3$) spectrum of *trans*,*trans*-2,4-hexa-dien-1-yl glycidyl ether (HDEGE, **1**). The complex structure of the NMR can be explained by the diastereotopic protons of the epoxide. All signals can be assigned and the integrals of the signals are in line with the expected values for the molecular structure. For detailed assignment see experimental section in the main manuscript.

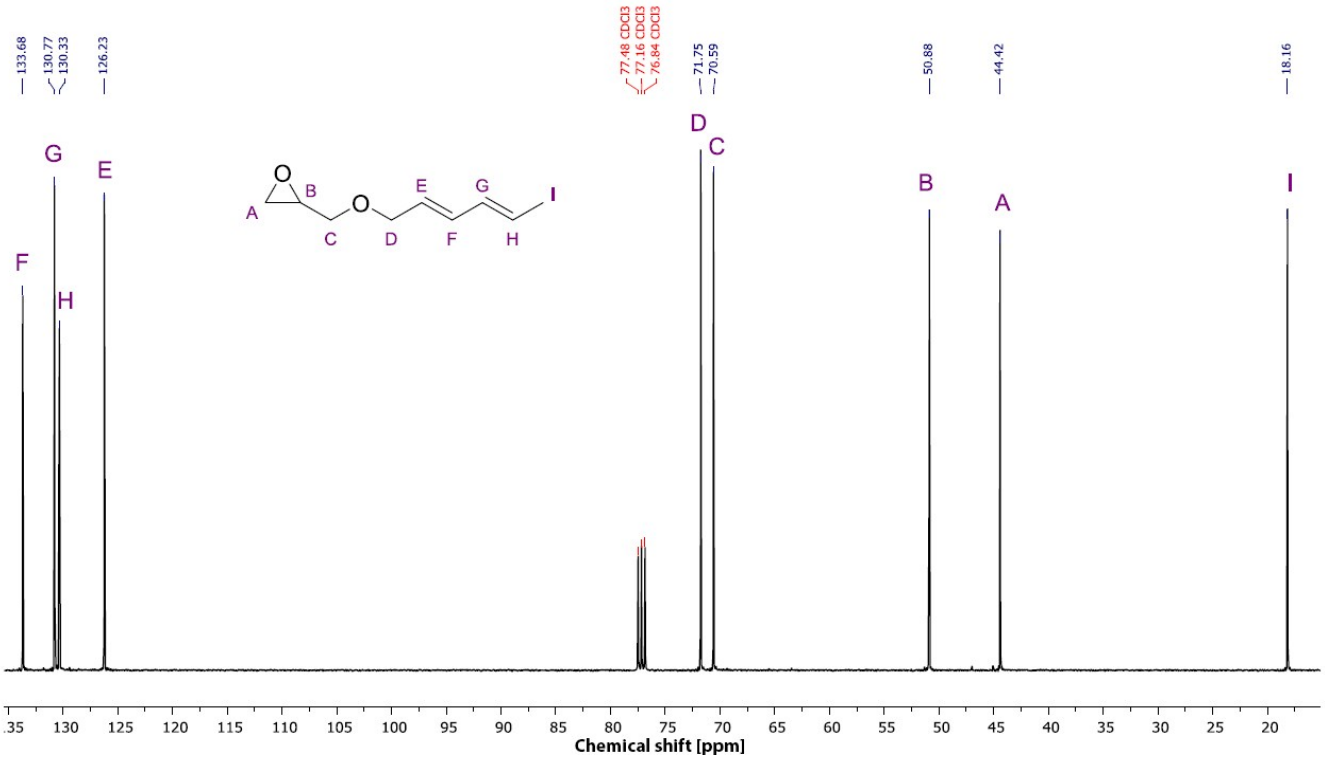

Figure S3b. ^{13}C NMR (100 MHz, $CDCl_3$) spectrum of *trans*,*trans*-2,4-hexa-dien-1-yl glycidyl ether (HDEGE, **1**).

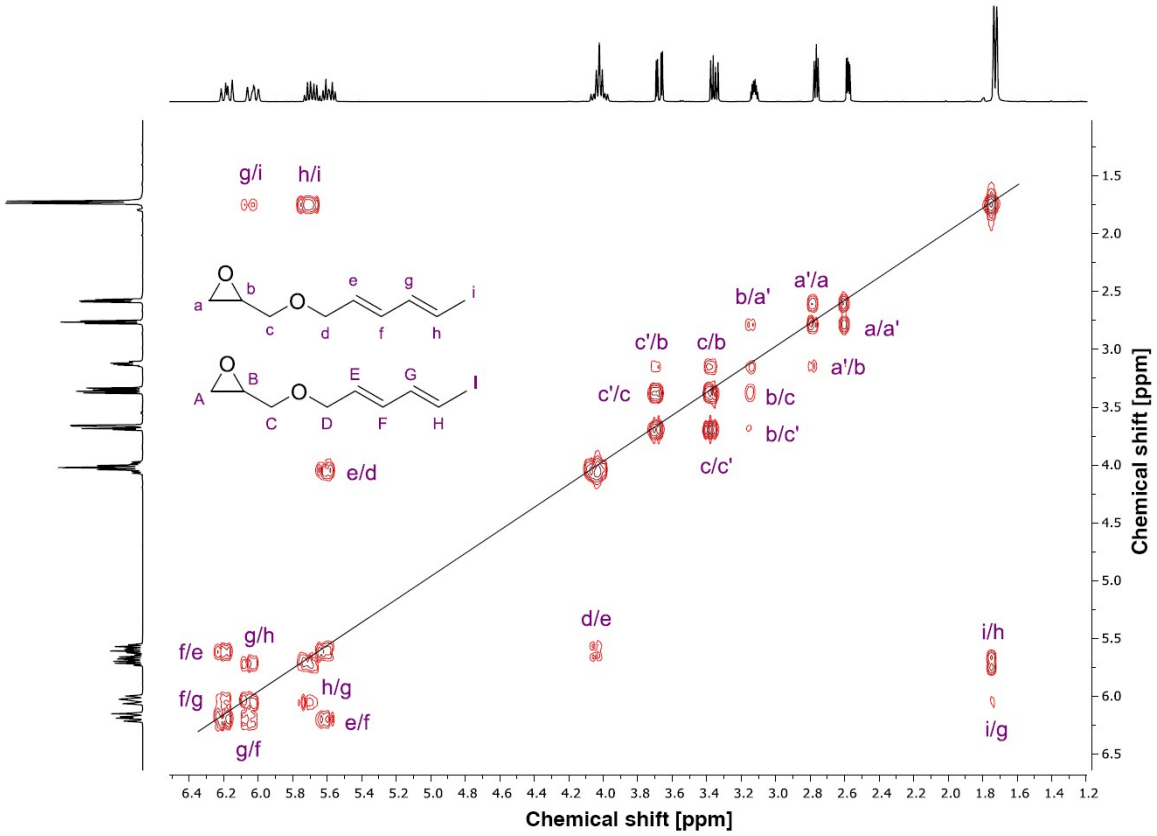

Figure S3c. ^{1}H-^{1}H COSY NMR (400 MHz, $CDCl_3$) spectrum of *trans*,*trans*-2,4-hexa-dien-1-yl glycidyl ether (HDEGE, **1**).

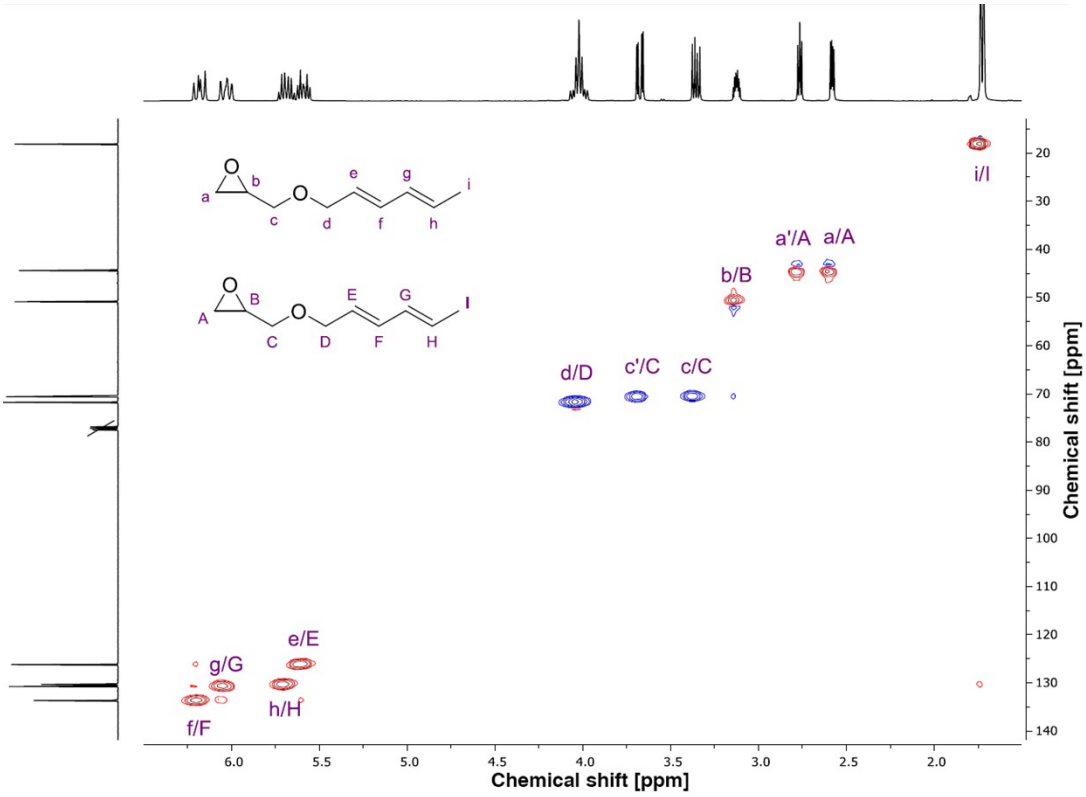

Figure S3d. ^{1}H-^{13}C HSQC NMR (400 MHz / 100 MHz, $CDCl_3$) spectrum of *trans*,*trans*-2,4-hexa-dien-1-yl glycidyl ether (HDEGE, **1**).

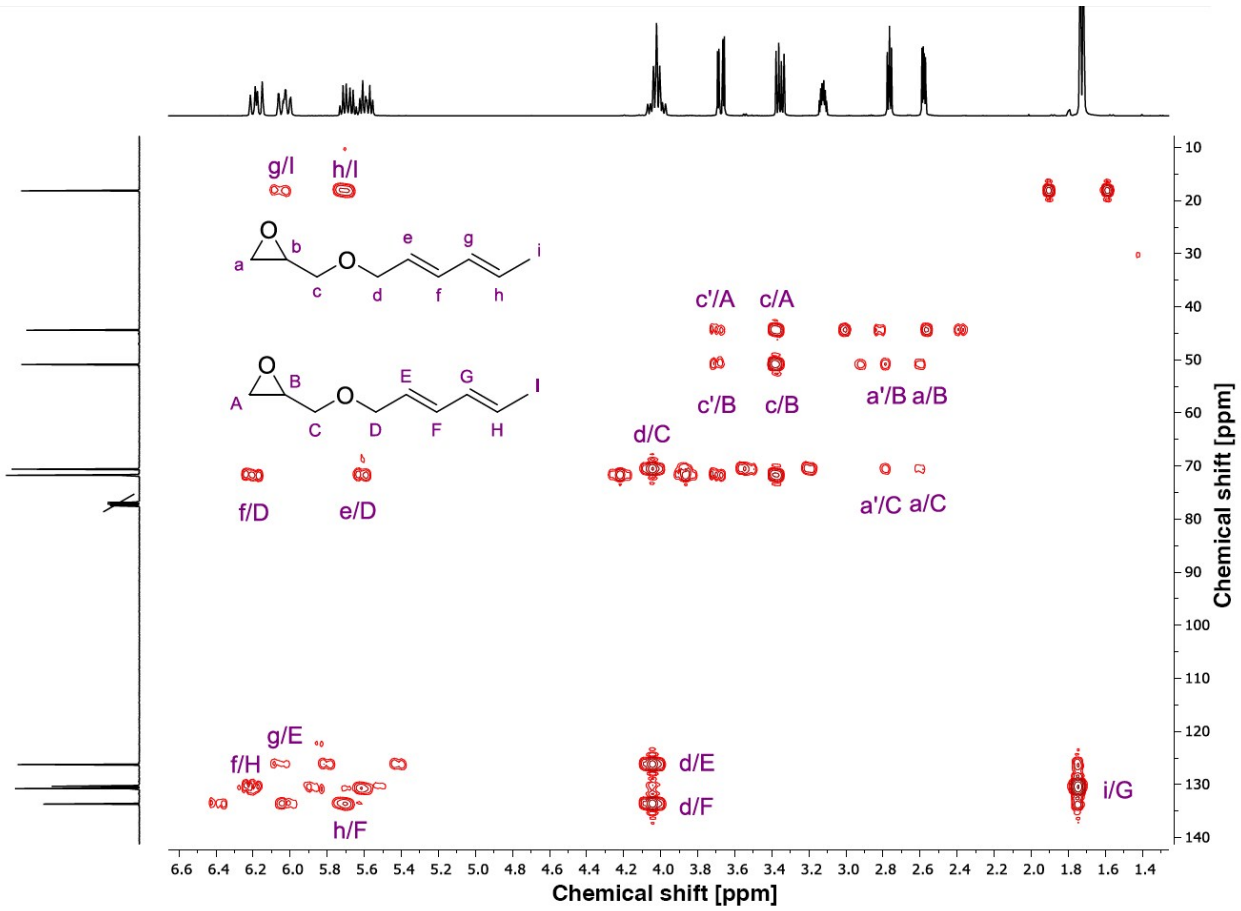

Figure S3e. ^{1}H-^{13}C HMBC NMR (400 MHz / 100 MHz, $CDCl_3$) spectrum of *trans*,*trans*-2,4-hexa-dien-1-yl glycidyl ether (HDEGE, **1**).

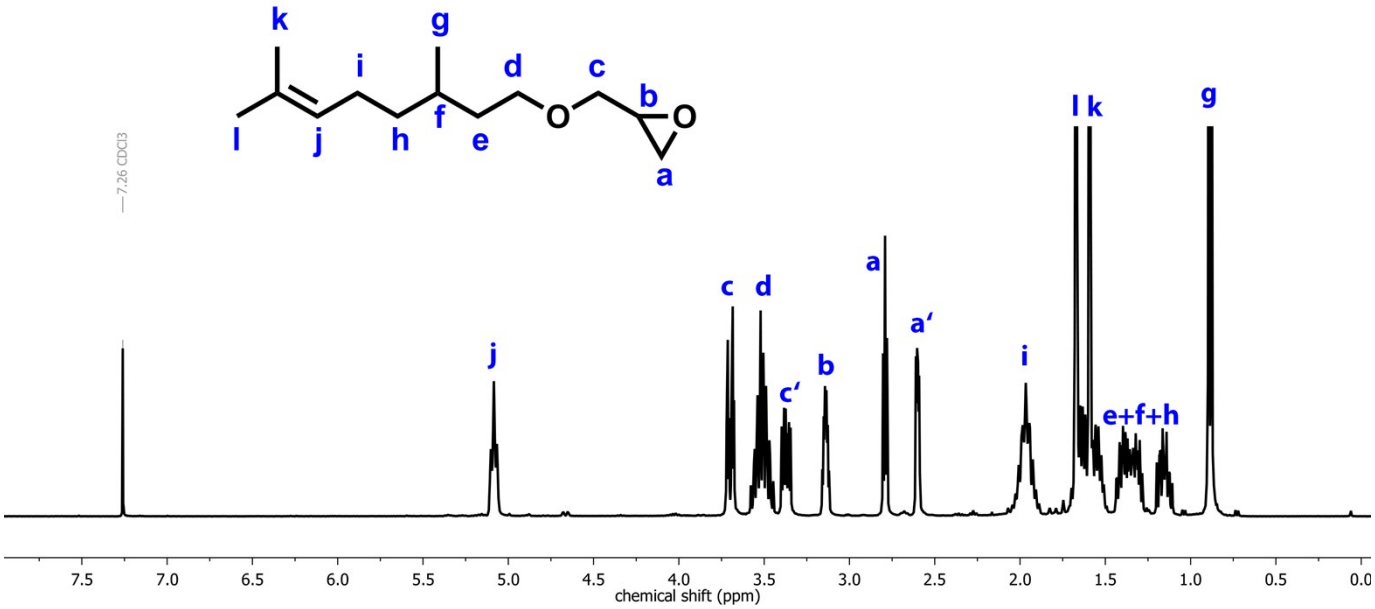

Figure S4a. ^{1}H NMR (400 MHz, $CDCl_3$) spectrum of citronellyl glycidyl ether (CitroGE, **2**). The complex structure of the NMR can be explained by the diastereotopic protons of the epoxide. All signals can be assigned and the integrals of the signals are in line with the expected values from the molecular structure. For a detailed assignment, see experimental section in the main manuscript.

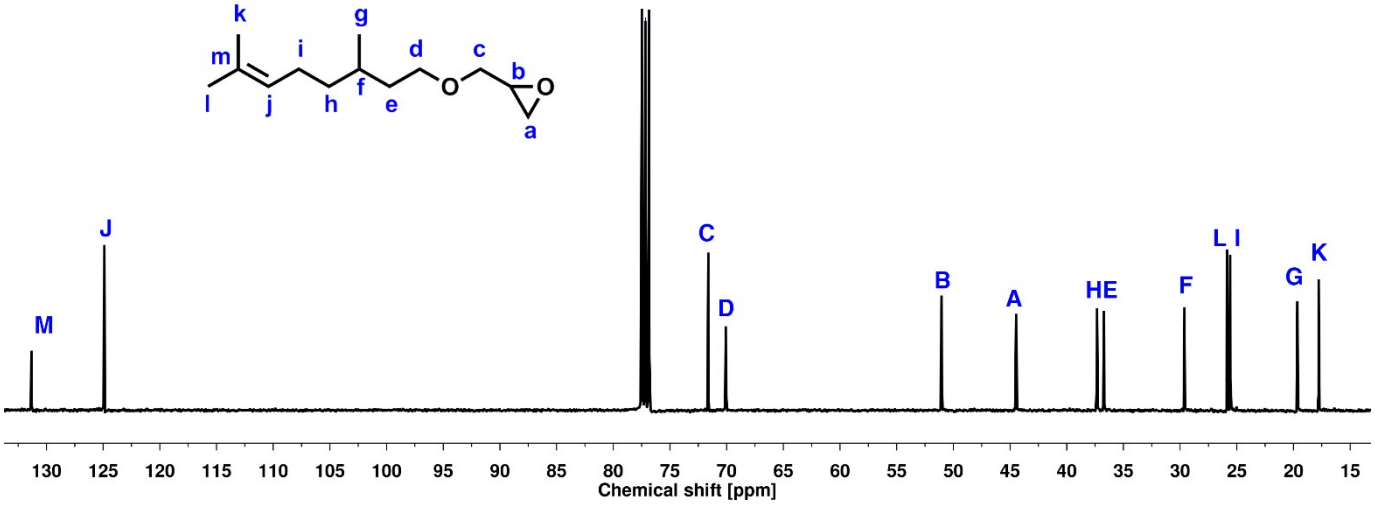

Figure S4b. ^{13}C NMR (100 MHz, $CDCl_3$) spectrum of citronellyl glycidyl ether (CitroGE, **2**).

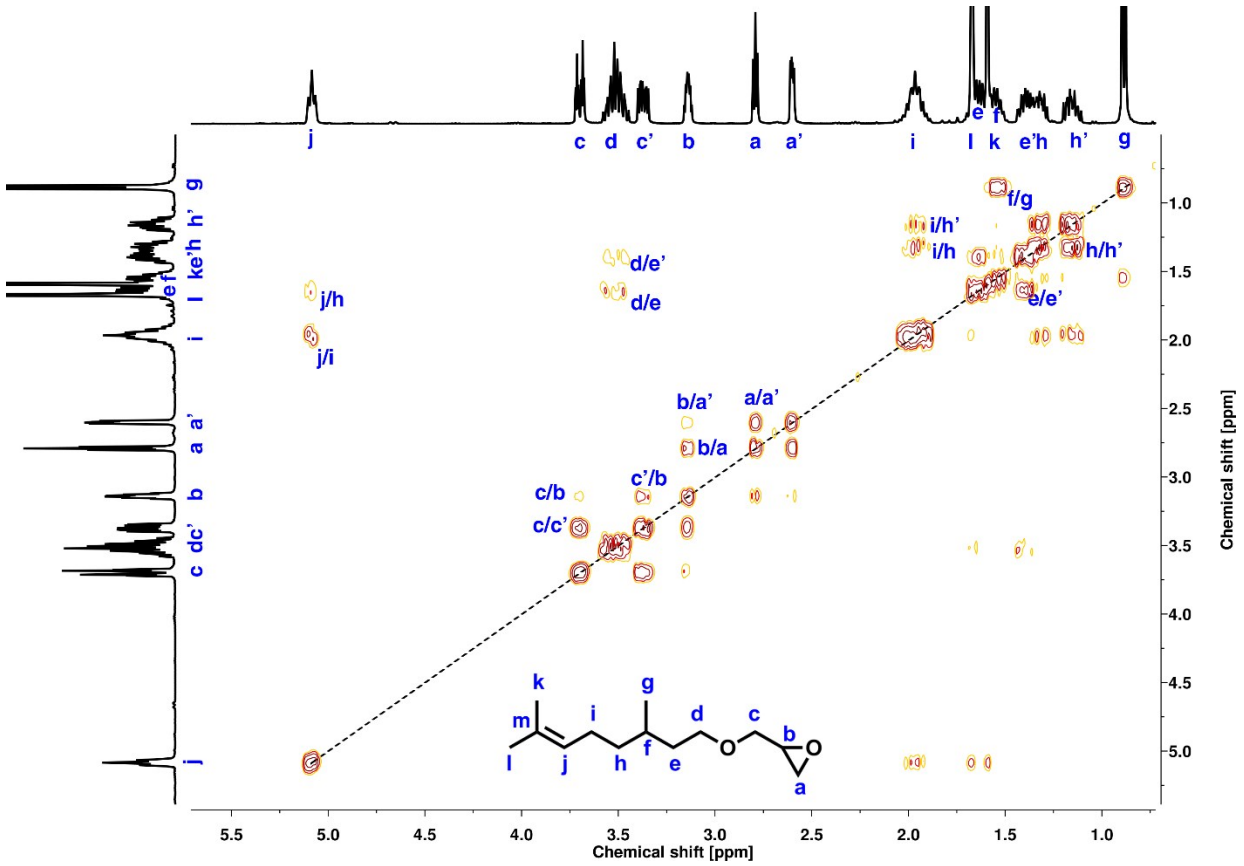

Figure S4c. ^{1}H-^{1}H COSY NMR (400 MHz, $CDCl_3$) spectrum of citronellyl glycidyl ether (CitroGE, **2**).

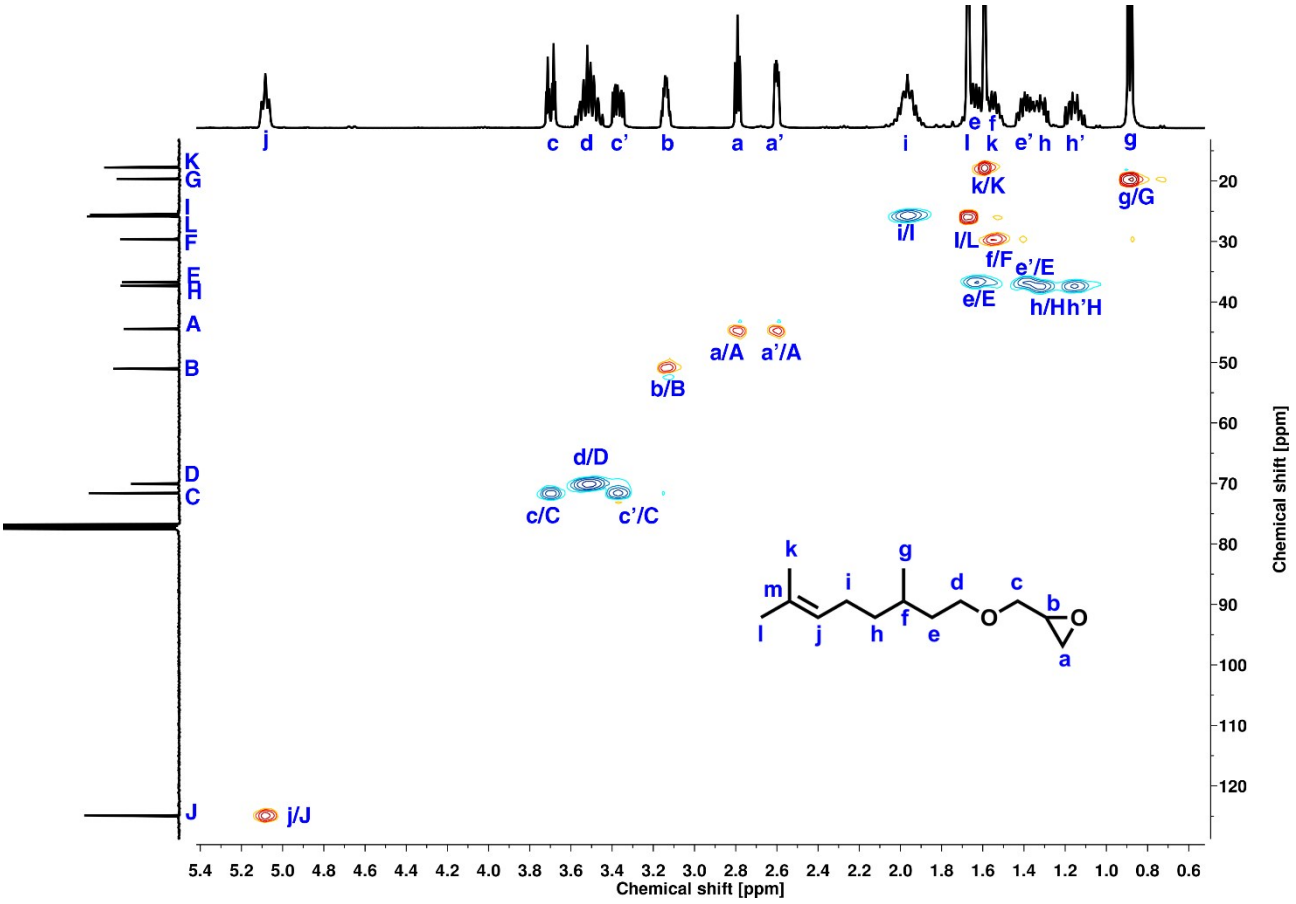

Figure S4d. ^{1}H-^{13}C HSQC NMR (400 MHz / 100 MHz, $CDCl_3$) spectrum of citronellyl glycidyl ether (CitroGE, **2**).

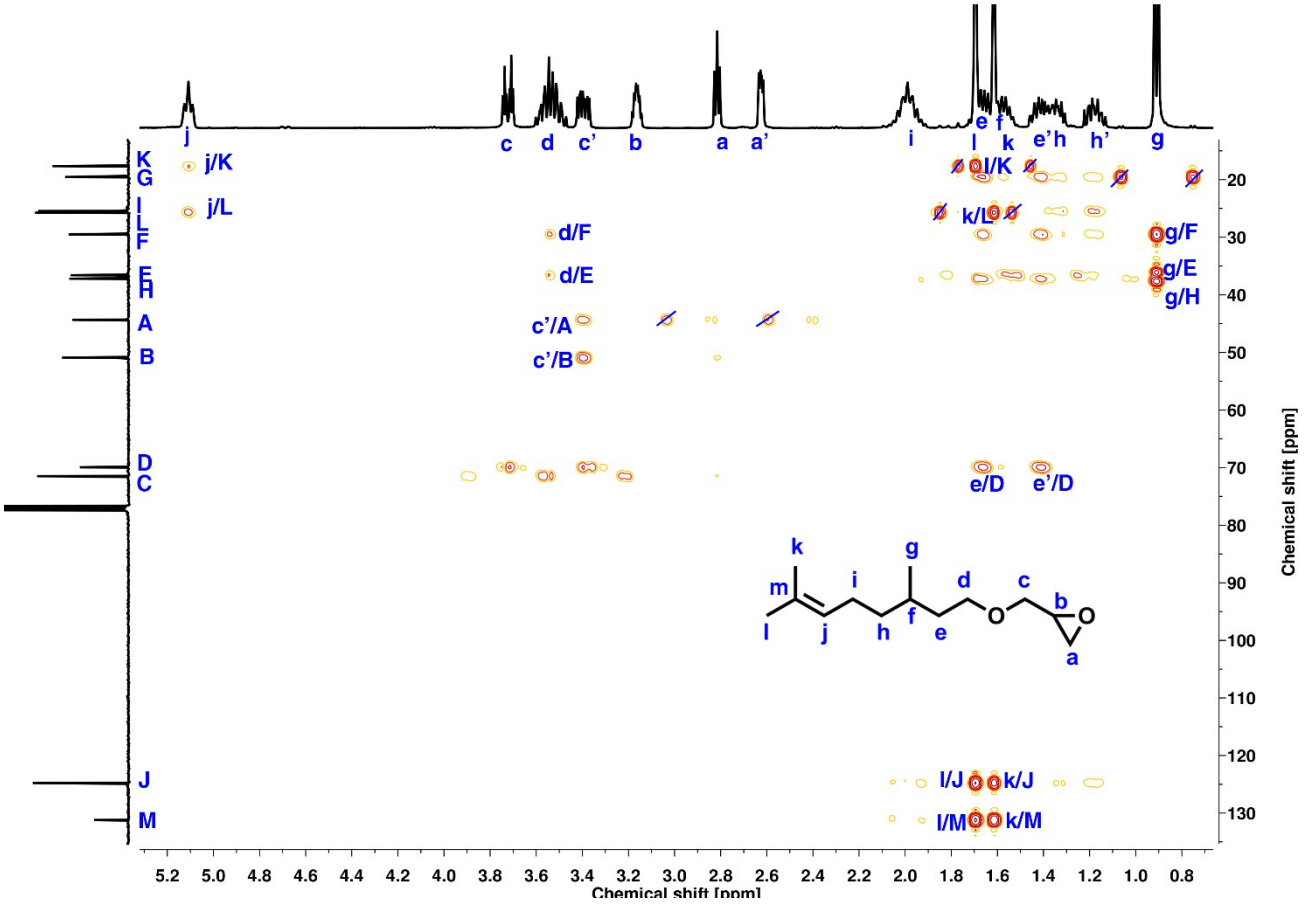

Figure S4e. ^{1}H-^{13}C HMBC NMR (400 MHz / 100 MHz, $CDCl_3$) spectrum of citronellyl glycidyl ether (CitroGE, **2**).) Only selected signals were assigned to maintain clarity of the assignment.

3. Characterization data of HDEGE based polymers

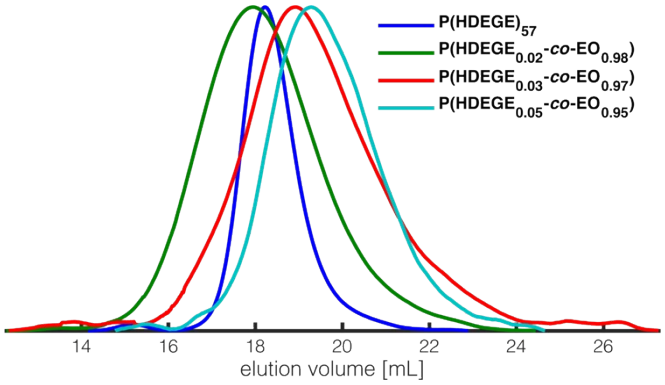

Figure S5. SEC traces (DMF, PEG calibration, RI detector) of PHDEGE and P(HDEGE-*co*-EO) polymers (**P1** and **P2**).

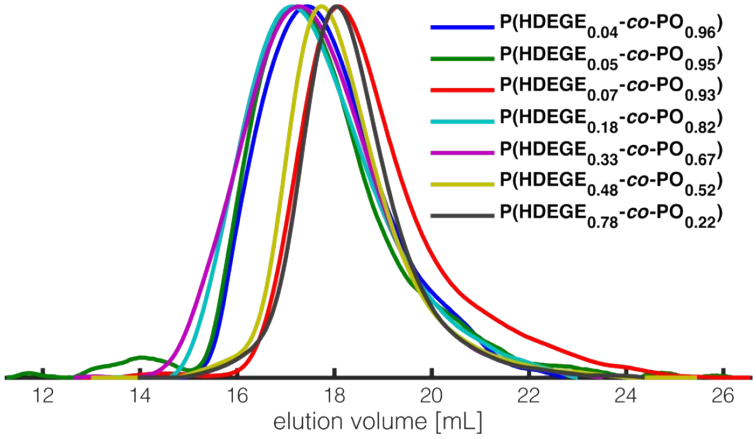

Figure S6. SEC traces (DMF, PEG calibration, RI detector) of P(HDEGE-*co*-PO) polymers (**P3**).

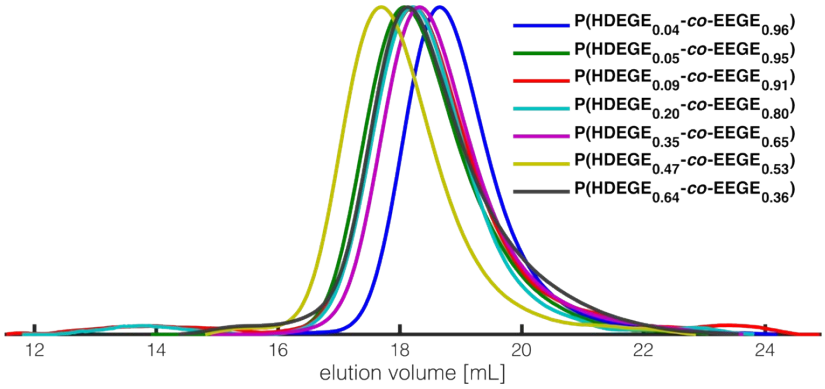

Figure S7. SEC traces (DMF, PEG calibration, RI detector) of P(HDEGE-*co*-EEGE) polymers (**P4**).

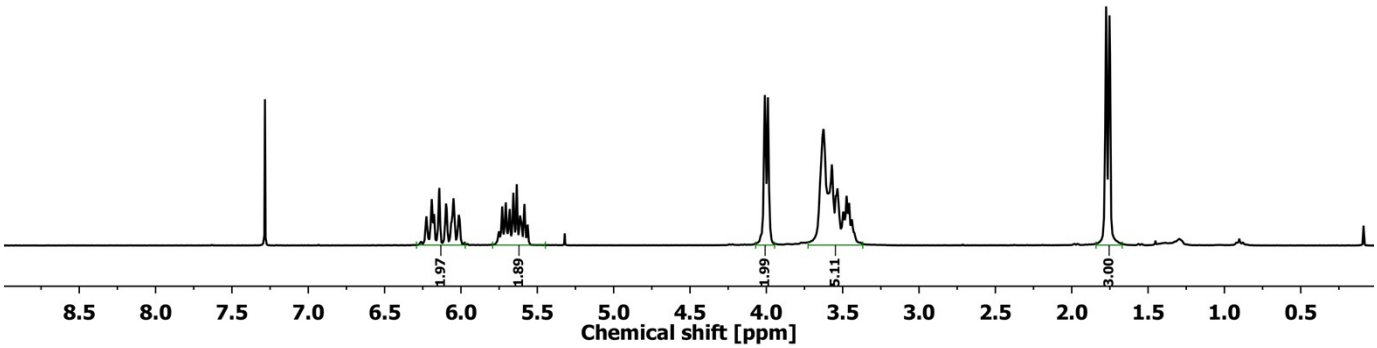

Figure S8. ^{1}H NMR (400 MHz, $CDCl_3$) spectrum of P(HDEGE) (**P1**). All signals can be assigned and the integrals of the signals are in line with the expected values from the molecular structure. For detailed assignment, see Figure 1.

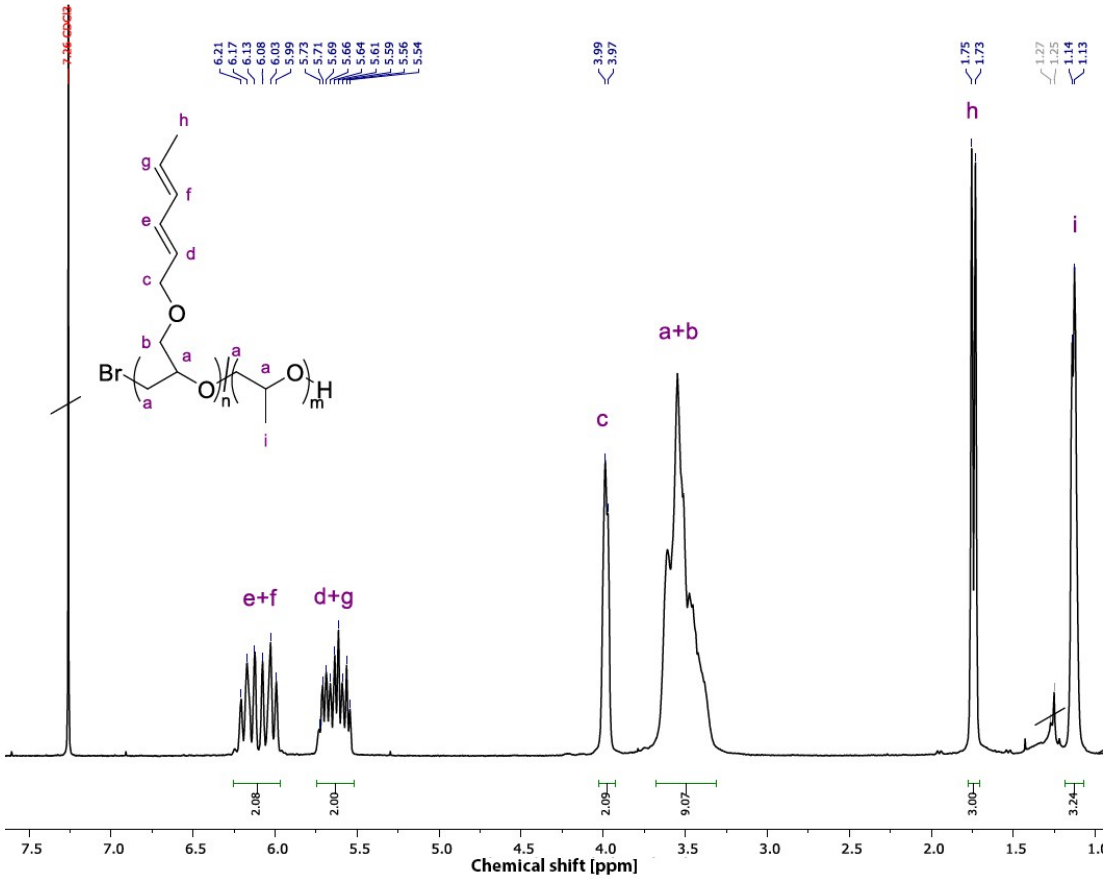

Figure S9. Exemplary ^{1}H NMR (400 MHz, $CDCl_3$) spectrum of P(HDEGE-*co*-PO) (**P3**). NMR spectra recorded for the P(HDEGE-co-EO) (**P2**) polymers (not shown) are analogous except for the CH_3 resonance at 1.14 ppm (signal i) that is not present in **P2**.

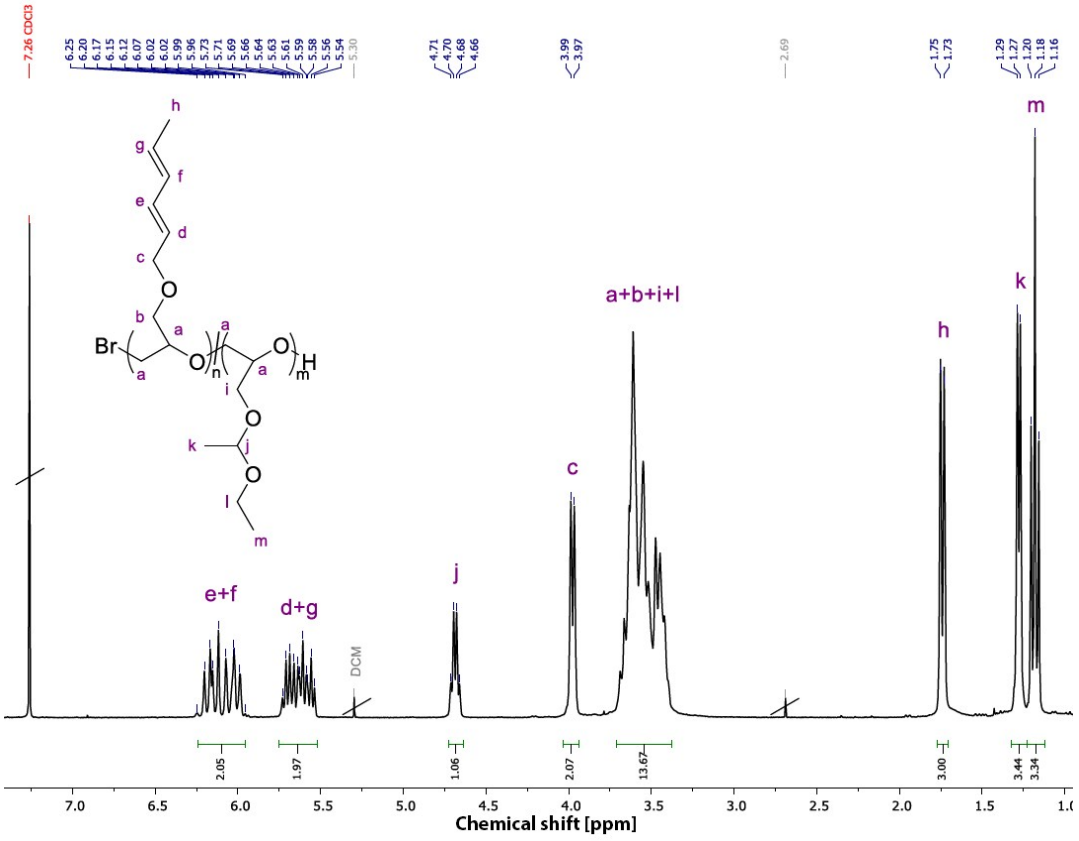

Figure S10. Exemplary ^{1}H NMR (400 MHz, $CDCl_3$) spectrum of P(HDEGE-*co*-EEEGE) (**P4**).

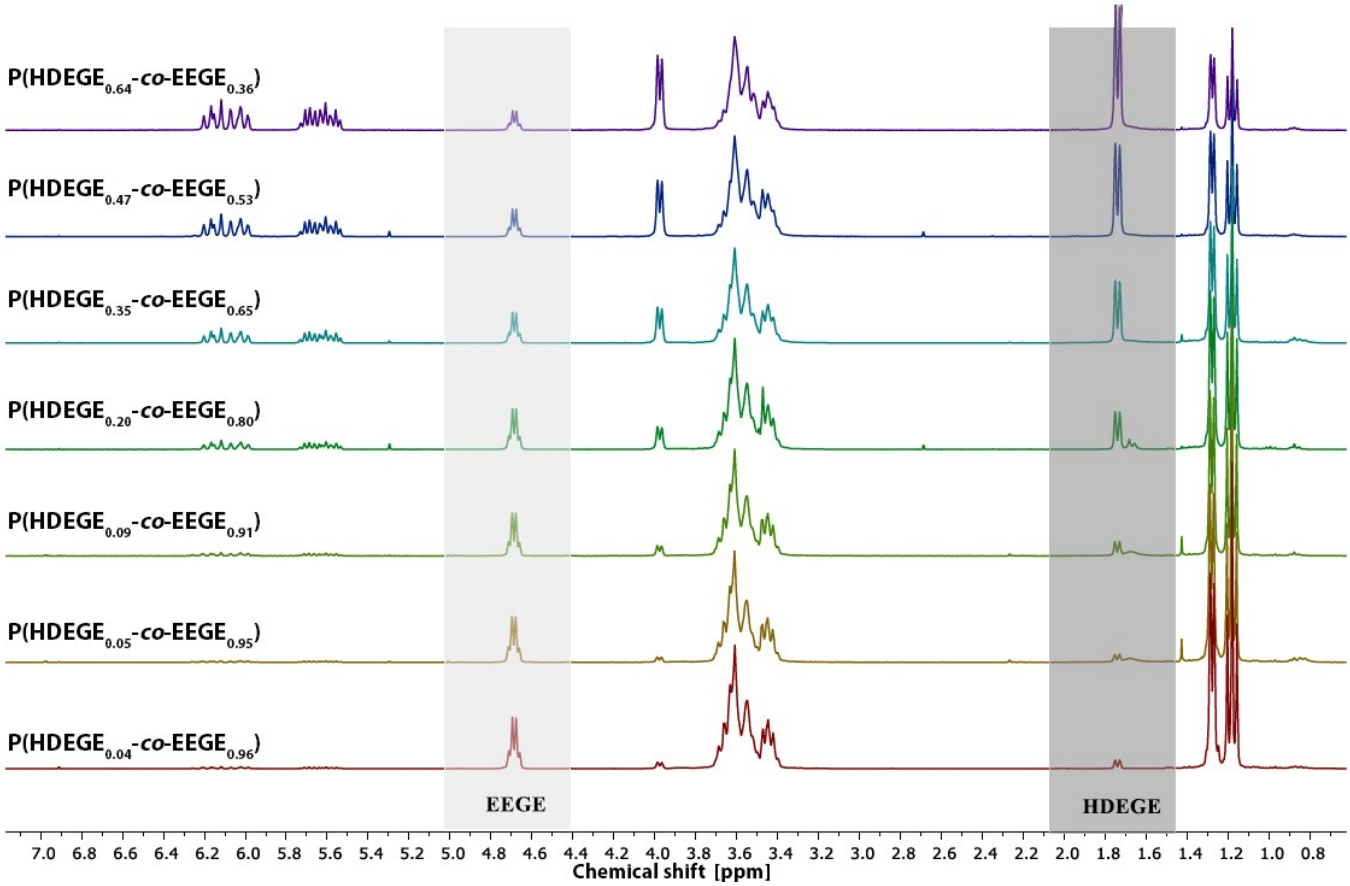

Figure S11. Stacked ^{1}H NMR (300 MHz, $CDCl_3$) spectra of all synthesised P(HDEGE-*co*-EEEGE) polymers (**P4**). The characteristic acetal proton for EEGE, as well the methyl group of HDEGE is highlighted. Polymer analysis via NMR shows excellent agreement of targeted and incorporated monomer ratios.

4. Characterization data of CitroGE based polymers

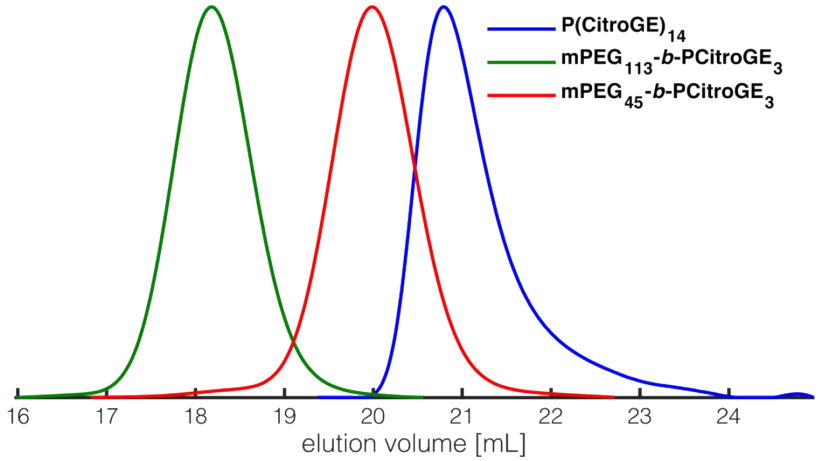

Figure S12. SEC traces (DMF, PEG calibration) of PCitroGE (**P5**) and mPEG-*b*-PCitroGE polymers (**P6**).

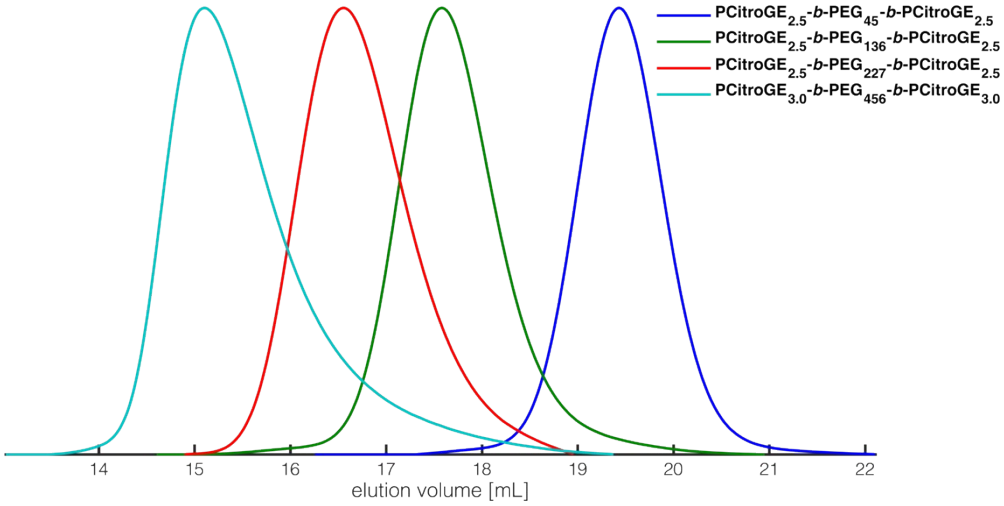

Figure S13. SEC traces (DMF, PEG calibration) of PCitroGE-*b*-PEG-*b*-PCitroGE polymers (**P7**).

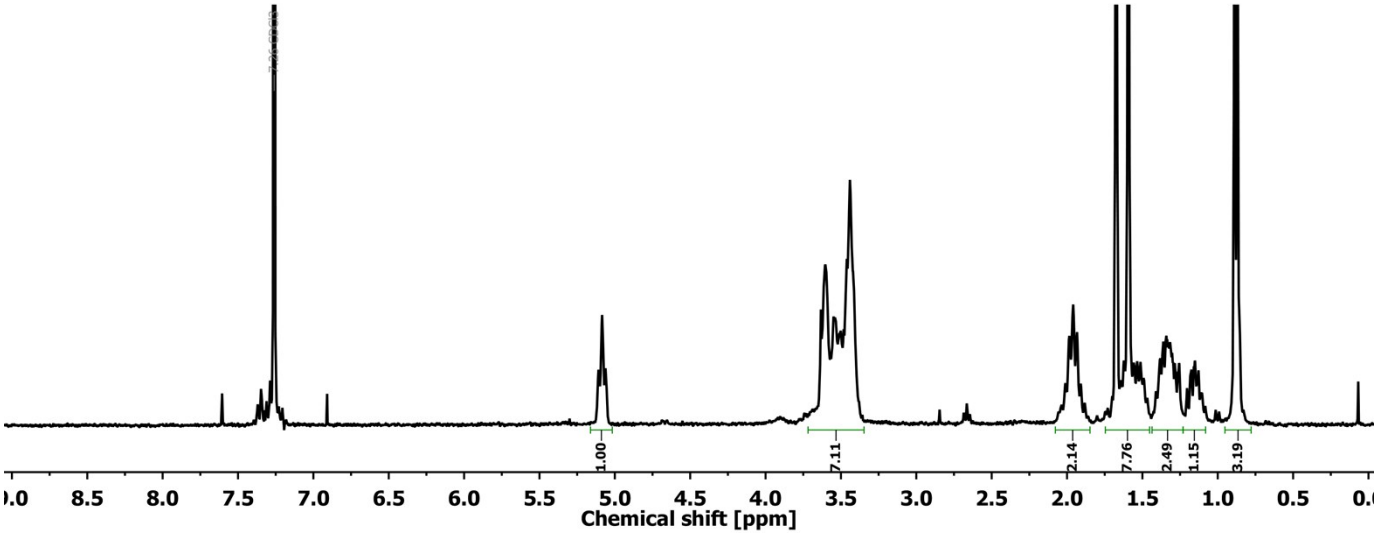

Figure S14. ^{1}H NMR (300 MHz, DMSO-d_6) spectrum PCitroGE$_{14}$ (**P5**). All signals can be assigned and the integrals of the signals are in line with the expected values from the molecular structure. For detailed assignment, see Figure 2.

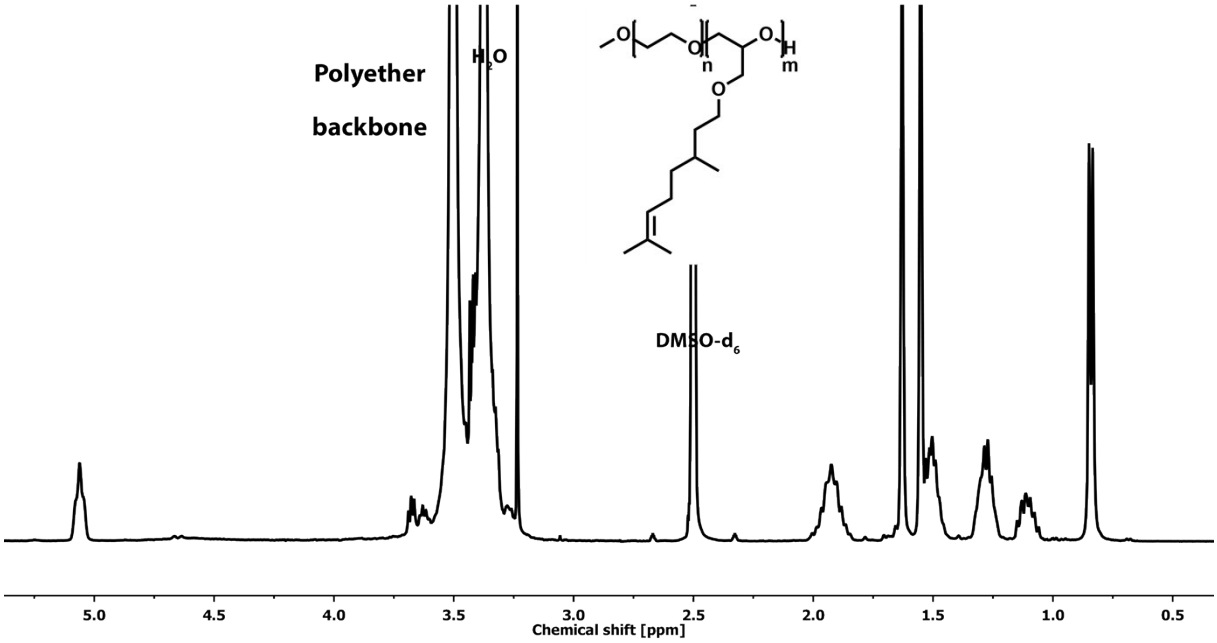

Figure S15. Exemplary ^{1}H NMR (300 MHz, DMSO-d_6) spectrum of mPEG$_{45}$-*b*-PCitroGE$_3$ (**P6**). ABA triblocks based on PEG show essentially the same NMR spectrum, except for the α-methyl group at 3.23 ppm.

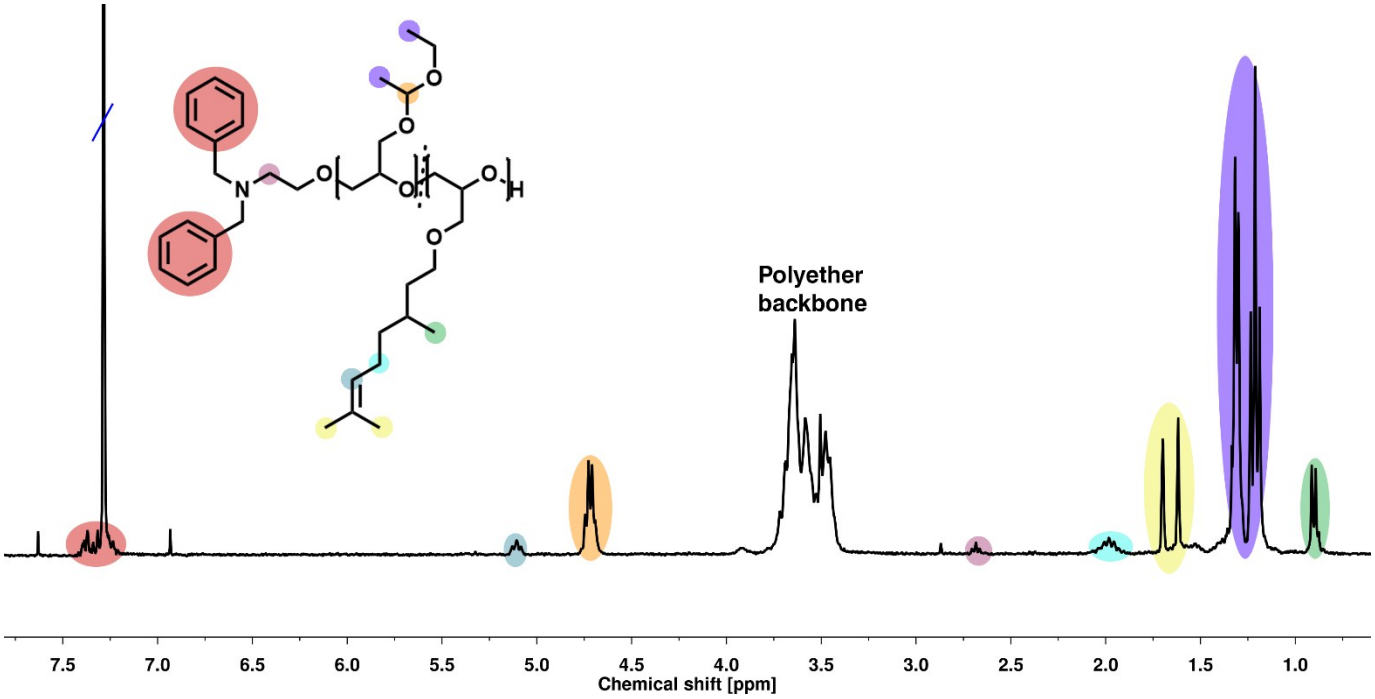

Figure S16. Exemplary ^{1}H NMR (300 MHz, $CDCl_3$) spectrum of P(CitroGE$_5$-co-EEGE$_{32}$) (**P8**).

5. Characterization data of functionalized polymers after TAD click

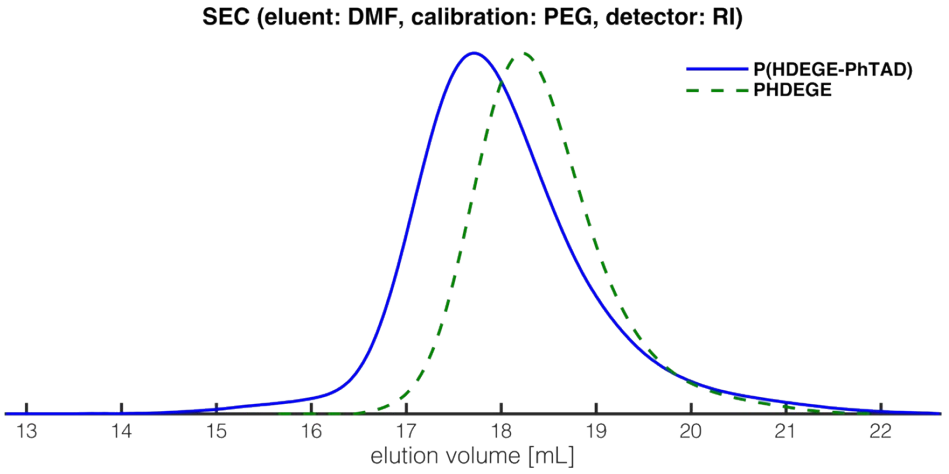

Figure S17. SEC traces (DMF, PEG calibration, RI detector) of PHDEGE (**P3**) before (green dashed line) and after functionalization with PhTAD (blue solid line).

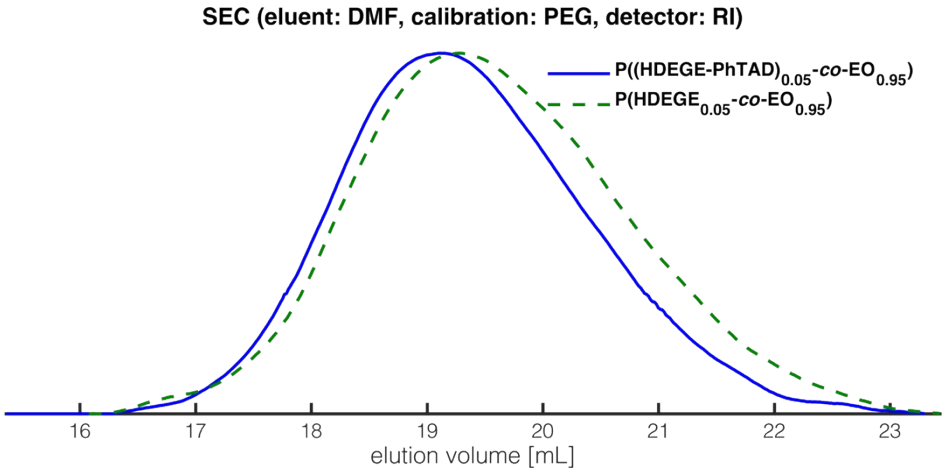

Figure S18. SEC traces (DMF, PEG calibration, RI detector) of P(HDEGE$_{0.05}$-*co*-EO$_{0.95}$) (**P2**) before (green dashed line) and after functionalization with PhTAD (blue solid line).

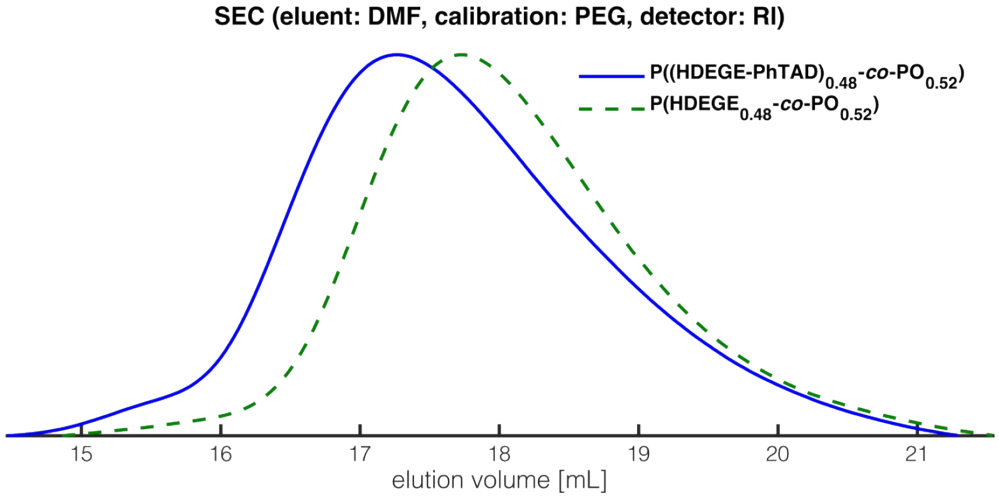

Figure S19. SEC traces (DMF, PEG calibration, RI detector) of P(HDEGE$_{0.48}$-*co*-PO$_{0.52}$) (**P3**) before (green dashed line) and after functionalization with PhTAD (blue solid line).

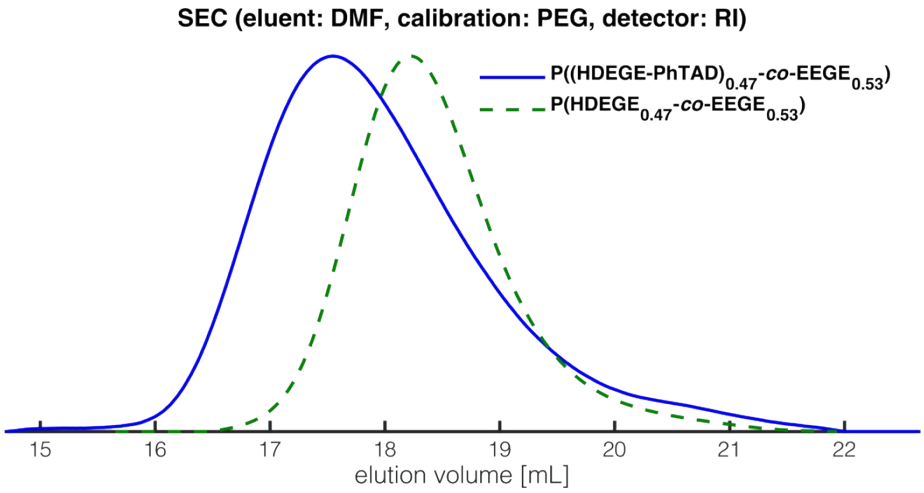

Figure S20. SEC traces (DMF, PEG calibration, RI detector) of P(HDEGE$_{0.47}$-*co*-EEGE$_{0.53}$) (**P4**) before (green dashed line) and after functionalization with PhTAD (blue solid line).

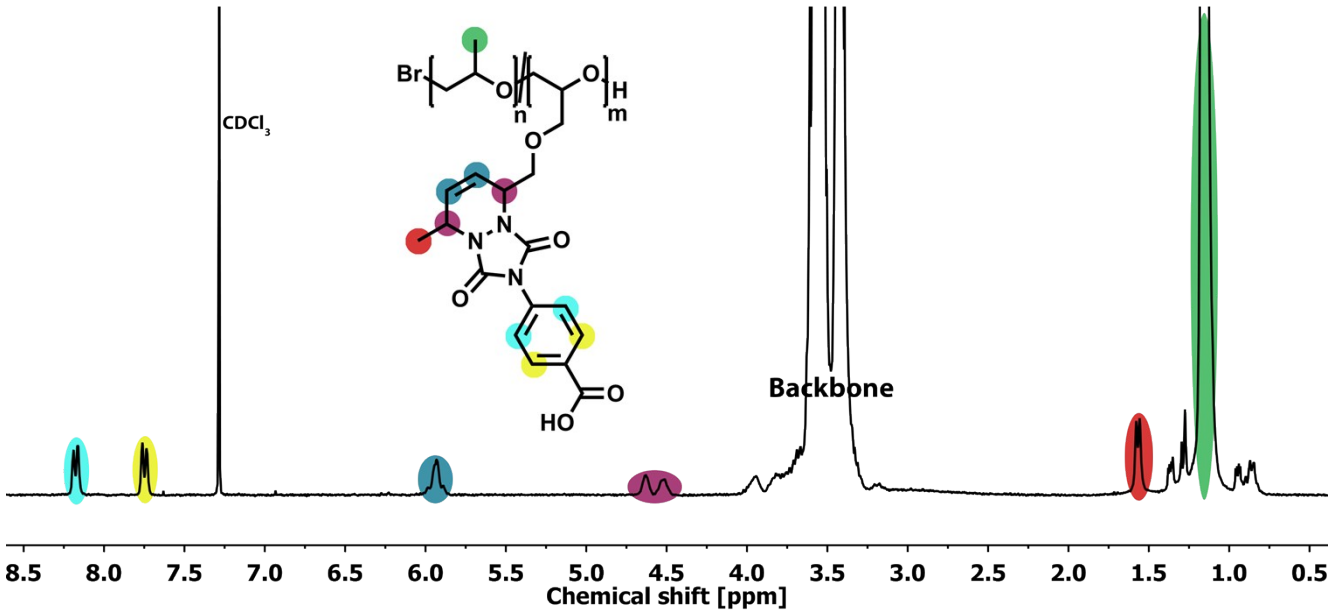

Figure S21. ^{1}H NMR (400 MHz, $CDCl_3$) spectrum of P(HDEGE$_{0.07}$-*co*-PO$_{0.93}$) (**P3**) after functionalization with HOOC-PhTAD. The success of the reaction is confirmed by the appearance of the typical AA'BB' spin-system of the para-substituted aromatic system.

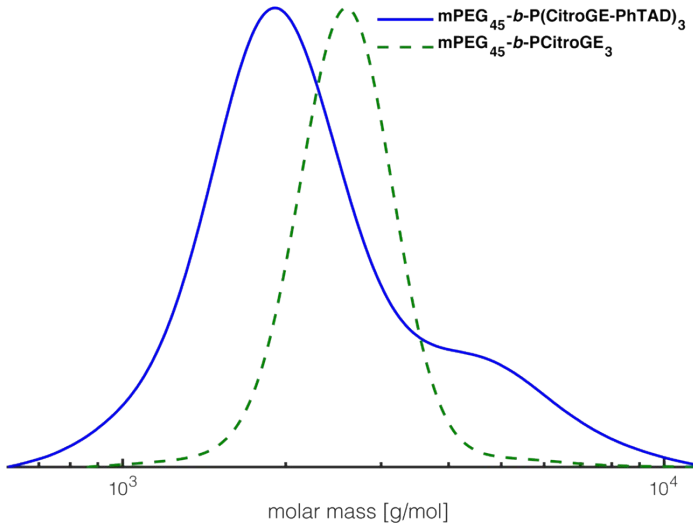

Figure S22. SEC traces (DMF, PEG calibration, RI detector) of mPEG$_{45}$-*b*-PCitroGE$_3$ (**P6**) before (green dashed line) and after functionalization with PhTAD (blue solid line).

6. Network formation

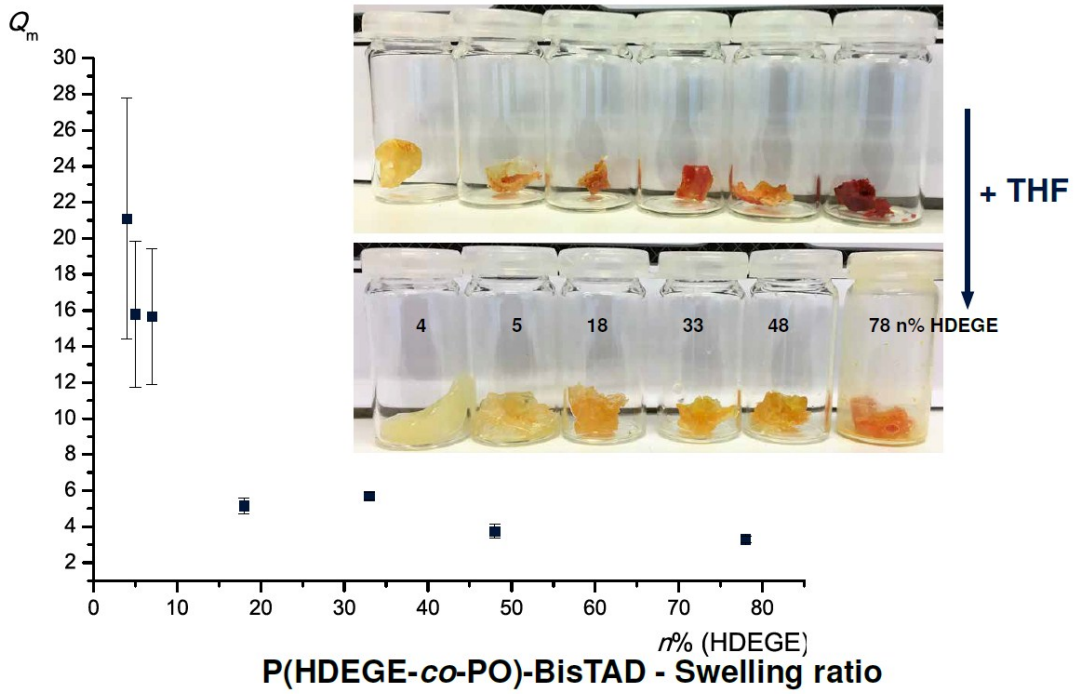

Figure S23. Swelling ratio of P(HDEGE-*co*-PO) polymers (**P3**) crosslinked upon bisTAD addition. With increasing HDEGE content, the crosslinking density also increases, leading to a reduced solvent uptake.

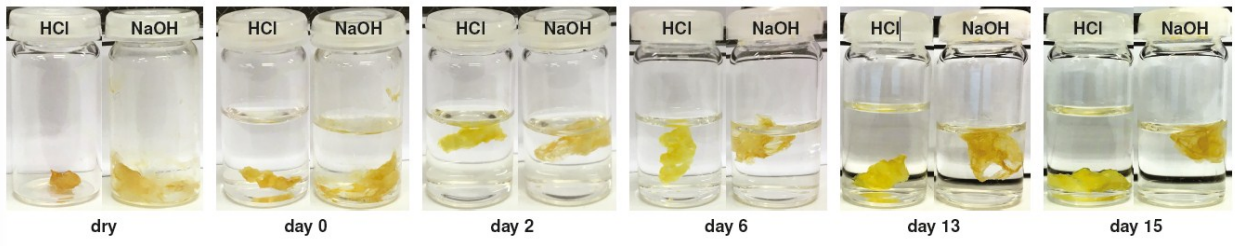

Figure S24. pH induced swelling of P(HDEGE-*co*-EEGE) polymers (**P4**) immersed in acidic aqueous solution (0.1 M HCl). The initial hydrophobic network is transformed into a hydrophilic linear polyglycerol-based network through acidic cleavage of the acetal protecting group. A similar experiment in aqueous NaOH (0.1 M) is shown and used as reference. In contrast to the swelling in HCl, no change in size or form of the material was observed in NaOH.

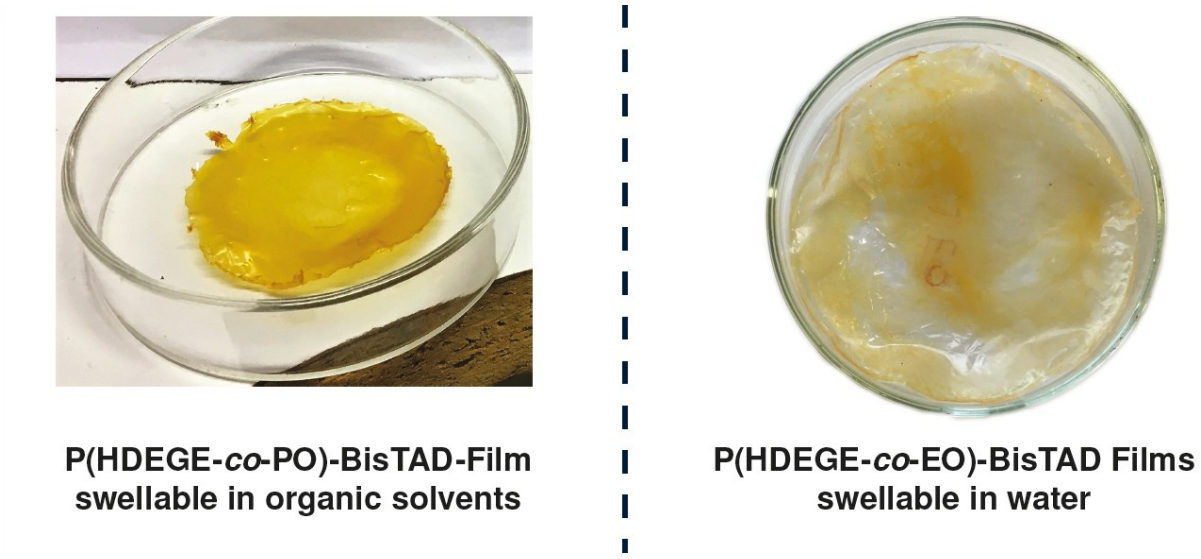

Figure S25. Films produced by addition of a bisTAD solution to a P(HDEGE-co-PO) (**P3**) and P(HDEGE-co-EO) (**P2**) solution, respectively. After instantaneous crosslinking, the materials were dried to obtain stable films. Films based on EO were swellable in water, while PO based films were swellable in common organic solvents.

References

1 a) A. Gandini, *Prog. Polym. Sci.*, 2013, **38**, 1–29; b) M. J. Barthel, T. Rudolph, S. Crotty, F. H. Schacher and U. S. Schubert, *J. Polym. Sci. A. Polym. Chem.*, 2012, **50**, 4958–4965; c) M. J. Barthel, T. Rudolph, A. Teichler, R. M. Paulus, J. Vitz, S. Hoeppener, M. D. Hager, F. H. Schacher and U. S. Schubert, *Adv. Funct. Mater.*, 2013, **23**, 4921–4932; d) J. Hilf, M. Scharfenberg, J. Poon, C. Moers and H. Frey, *Macromol. Rapid Commun.*, 2015, **36**, 174–179;

2 K. Hoogewijs, D. Buyst, J. M. Winne, J. C. Martins and A. Madder, *Chem. Commun.*, 2013, **49**, 2927–2929.